In: SPIE Optical Metrology 2023: Optical Measurement Systems for Industrial Inspection XIII,
26-29 June 2023, Munich, Germany. Volume 12618, Paper number 126181G
DOI:10.1117/12.2673177

Application and performance of laser speckle odometry applied to a mobile industrial robot

Thomas O.H. Charrett[a*], Sam J. Gibson[a], and Ralph P. Tatam[a]

[a]Centre for Engineering Photonics, Cranfield University, MK43 0AL, UK.

ABSTRACT

In this paper we report the application of a laser speckle odometer to a mobile industrial robot in a typical factory floor environment. The suitability of typical floor surfaces and features is assessed in terms of the ability to form speckle patterns with sufficient signal to noise for correlation-based processing. All tested surfaces including concrete, rubber tile, dried paint and oil stains, and hazard tapes were found to be suitable. A comparison of the velocimetry sensor output to the industrial robot's internal SLAM and wheel encoder data is presented with good agreement of < 0.3mm/s at tested speeds of up to 250mm/s. Finally, a comparison of speckle odometry to the robot's internal SLAM based navigation will be presented using a laser tracker to provide ground-truth measurement data. Both techniques were found to perform similarly, with errors of up to 80mm when traversing a 16m square path of 4m sides. The laser speckle odometry was however found to perform significantly better over the initial sides of the path with a maximum error of < 10mm in comparison to < 47mm for the robot's internal odometry.

Keywords: Laser speckle, robotic odometry, mobile industrial robot

1. INTRODUCTION

Mobile industrial robots are increasingly important for multiple areas of manufacturing and automation; offering the ability to fully utilise robot resources by moving between production cells[1] or for the manufacturing of large objects for example in aerospace, wind turbine manufacturing[2] or large area additive manufacturing such as in construction.[3]

Current navigation approaches predominately rely on a combination of laser scanner, inertial measurement unit (IMU) and wheel encoder data together with simultaneous localisation and mapping (SLAM). However, this approach may have insufficient accuracy or be unreliable due to environmental conditions such as featureless areas or constantly changing areas where mapping becomes unreliable.[4] Alternative approaches such as laser beacon-based systems, for example iGPS, require multiple beacons and line-of-sight to be maintained,[2] while radio frequency Identification (RFID) or visual tags again require installation and maintenance of navigation markers which may not always be possible or desirable.[5]

Laser speckle odometry[6–8] is a non-contact optical method of measuring the real robot motion using a ground-facing camera and laser illumination, along with image correlation-based processing. The approach offers potentially high-quality complimentary data about the robot's motion to that provided by wheel encoders and has several advantages; it is insensitive to errors from wheel wear and skidding, and hence can be applied to non-wheeled, tracked or walking robots[7] and it provides both forward and lateral velocities. However, previous work has focused on niche application areas[6,7] or the application of optical computer mice in robotics laboratories.[8] Here we report the application of a laser speckle odometer to a MIR200 mobile industrial robot in a typical factory floor environment. The suitability of typical floor surfaces and features and a comparison of speckle odometry to the robot's internal SLAM based navigation will be presented using a laser tracker (Leica absolute tracker AT960-XR) to provide ground-truth measurement data.

*corresponding author: T.O.H. Charrett: E-mail:t.charrett@cranfield.ac.uk

Published by SPIE. Issued with: Creative Commons Attribution License (CC:BY 4.0).
The final published version (version of record) is available online at DOI:10.1117/12.2673177. Please refer to any applicable publisher terms of use.

2. EXPERIMENTAL EQUIPMENT

2.1 MIR200 industrial robot

To trial the application of speckle odometry in an industrial setting a MIR200 Autonomous mobile robot was used, see Figure 1. This robot is designed for small/medium transportation tasks within industry logistics[9] and can transport up to 200kg with a maximum speed of 1.1m/s. It is equipped with two laser scanners mounted on the front and back at opposite corners for 360° coverage and navigates using a SLAM algorithm with a quoted positioning accuracy of ±50mm under controlled conditions.[9] Access to the internal navigation data was limited to an http network interface, this allowed logging of the robot's internally calculated position and speed at approximately 10Hz with data logged to a laptop connected to the MIR robot's internal WiFi interface.

2.2 Laser speckle sensor

In our previous work[6,10] we have previously focused on the use of lensless objective speckle, to maximise light collection and reduce system complexity. Here we choose instead to use an imaging geometry with subjective speckle, due to the fixed working distance requirements and subsequently higher expected signal levels. This has the advantages of allowing a higher maximum velocity via selection of the magnification, and insensitivity to tilt (pitch & roll) motions. The sensor head, shown in Figure 2, consisted of a laser diode module (Global laser ACCULASE-PWM-650-5-S, 650nm, 5mW max output) and beam shaping lens producing an elliptical spot ∼ 15x10mm. The laser was modulated at 500Hz with a 20% duty-cycle to limit the accessible emission to laser class I for eye-safety and to prevent blurring of the speckles. As an additional safety precaution, the laser spot and sensor head were enclosed by a flexible rubber skirt which also served to reduce background light levels.

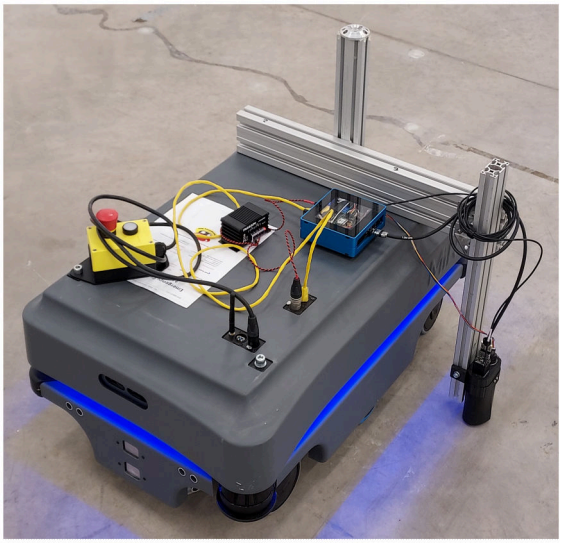

Figure 1: Photograph of the MIR200 robot

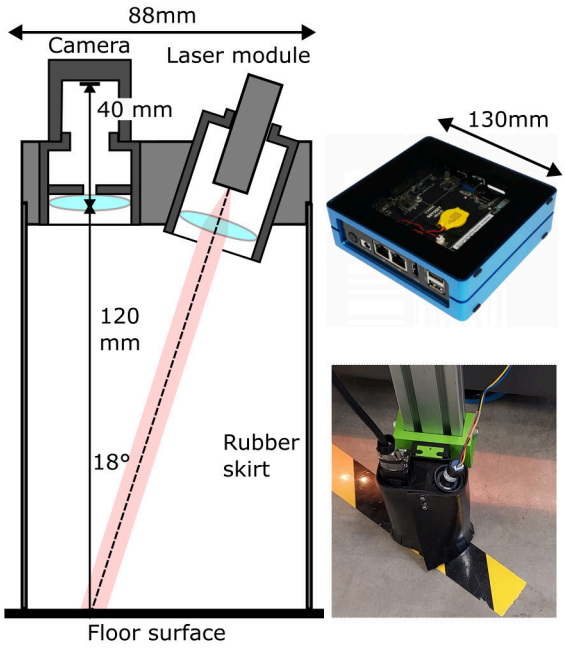

Figure 2: Schematic of laser speckle sensor head (left) and photograph (bottom right) and the mini PC used for signal processing (top right)

The illuminated surface was imaged via a low-cost aspheric lens (f=30mm, Thorlabs AC254-030-AB) onto a USB3 industrial camera (Ximea MQ013RG-ON) operating at 500fps with an image size of 512x512 pixels. Pairs of images were acquired and processed at either 50Hz or 100Hz depending upon the test. Careful selection of frame-rate (inter-frame time), aperture size and image magnification is necessary to ensure successful operation: a $d_{ap} = 5$mm aperture was located just behind the lens to produce speckles of approximately $2-3$ pixels as required for optimal correlation peak-fitting.[10] For the camera frame rate and maximum speed of the robot the

maximum resulting surface translation would be 2.2mm, which is below the limit imposed by the aperture size of $\sim d_{ap}/2\text{mm}$[11] beyond which the speckle patterns decorrelate. Finally, image magnification was set to 0.33 giving a resulting speckle translation on the camera of 0.7mm or 152 pixels which again is less than the limit imposed by the image size and correlation processing that restricts shifts to ± half of the image size.

A mini PC with integrated Arduino micro-controller (Seeed Odyssey Intel Celeron J4105) was used to control laser modulation and synchronise camera triggering and perform the laser speckle correlation processing.[10] The calculated velocimetry data was then stored to the mini PC's SSD drive; the odometry calculations requiring both MIR robot orientation and speckle velocimetry data were performed in post processing. Additionally, for some experiments the raw speckle images were stored allowing post-processing and analysis.

2.3 Laser tracker & test environment

To provide ground-truth reference data and allow an assessment of both MIR robot SLAM navigation and laser speckle odometry a laser tracker (Leica absolute tracker AT960-XR) was used to continuously track a reflector located on top of the MIR robot. This laser tracker has a maximum permissible error of 14um at the range of < 10m used here. The test environment was a working factory floor/workshop environment with predominately sealed concrete floor, with areas of rubber tiles and hazard/marking tapes and expansion gaps. The sensor was tested on a variety of these different floor surfaces. A pre-generated map of the workshop was used for the MIR navigation, however several pieces of equipment had been moved between generation of the map and the trials, offering a good test of the real-world performance of the MIR's SLAM navigation.

3. RESULTS

3.1 Velocimetry results

The initial tests focused on the suitability of different floor surfaces for speckle measurements, by recording short sequences it was found that the speckle sensor worked well on all floor surfaces, with only changes in the overall signal intensity. All tested surfaces including concrete, rubber tile, dried paint and oil stains, and hazard tapes were found to be suitable. For example, Figure 3a shows a black and yellow safety tape with the resulting speckle pattern shown in Figure 3b. This frame shows the transition between the two tape colours and the resulting signal level change with the yellow tape showing as the high signal region in the bottom-left corner. The inset axis of Figure 3b shows a region of the black tape where the colour scaling has been adjusted to show the presence of the speckle pattern. As laser speckle correlation processing is not directly an intensity-based technique, so long as laser speckles are visible the pattern shift can be determined and there was no failure in correlation for this and other low reflectivity surfaces. However, it is likely that lower signal-to-noise will influence the accuracy of the peak fitting process.

(a) (b)

Figure 3: Example (a) photograph of surface feature and (b) resulting speckle pattern for black and yellow safety tape. Inset is contrast enhanced region of the black tape showing presence of speckle pattern for correlation.

An example of the measured velocity is shown in Figure 4 for a commanded 4m forward drive of the robot at 0.25m/s, which was then followed by a 90° turn on the spot. Here the output of the speckle velocimeter is shown as blue/green data points for the v_x and v_y components respectively, after the application of a 0.2 second

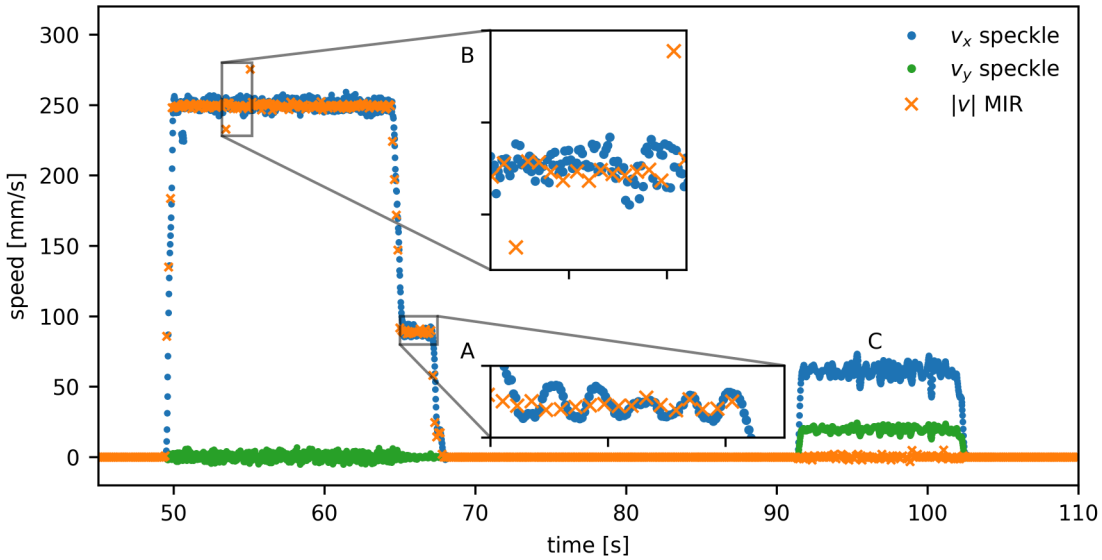

Figure 4: Comparison of the velocity signals from the laser speckle sensor with the MIR robot's reported speed from a combination of SLAM and wheel encoder data. Label A shows resolution of velocity oscillations, Label B shows jumps in MIR reported position likely corresponding to SLAM position adjustments, and Label C shows velocity components associated with 90° on the spot rotation due to speckle sensor offset from the centre of the robot.

averaging filter. For comparison, the robot's internally reported speed, $|v|$, is shown by the orange crosses. There is very good agreement, < 0.3mm/s, between the two data sets, including a deceleration from 250mm/s to around 100mm/s that occurred around 65 seconds (labelled A on the plot). Around this point the inset axis shows that the speckle measurements can also clearly resolve oscillations/control of the robots speed, which are not visible in the combined SLAM/wheel encoder data reported by the MIR robot. A second interesting feature can be seen in the inset axis at label B, where two sudden jumps in the speed reported by the MIR robot can be observed; this appears to be caused by a readjustment to the robot's position from SLAM data and can also been seen by jumps in the reported position. Finally, at label C on the plot, the v_x and v_y velocity components caused by the 90° rotation and the offset of the sensor from the robots centre point can be seen highlighting the sensors ability to provide velocimetry in 2-axes. The MIR robots reported speed fluctuates about zero during this period as the robot's frame-of-reference is located at, or close to, the centre-of-rotation.

3.2 Odometry results

The velocity output of the speckle sensor can then be integrated to perform simple odometry which can be compared with the MIR robot's internal odometry based on a combination of wheel encoder and SLAM data, and both compared to the reference position data acquired continuously along the robot's path. Figure 5 shows calculated position results for a 16m square path with 4m sides, after coordinate transformation of the MIR robot odometry and laser speckle odometry data to the laser tracker reflector frame-of-reference. After each 4m drive, the robot rotated 90° on the spot, and as the reflector is offset from the robot's centre-of-rotation this appears as the arced path. Figure 5 A shows the start (0m) and end positions (16m) with a final offset of around 16mm for MIR odometry and 8mm using speckle odometry. However, for other datasets the errors for both could be up to $\sim$ 80mm. This is shown in Figure 6 which shows the mean errors for six runs around the 4m square path in the clockwise and anticlockwise directions with the error bars showing the minimum and maximum observed error. Generally, the speckle odometry performed better over the initial legs of the path; for example, Figure 5 B and C show excellent agreement with the laser tracker data and Figure 6 shows a maximum error of $<$ 10mm after 4m travel compared to $<$ 47mm for the internal odometry. This suggests that speckle odometry may be useful in improving the quality of SLAM mapping. Figure 5 C also shows a position update via the SLAM navigation leading to a jump to better position estimate, such jumps lead to the velocity spikes

shown in Figure 4 B. Finally the performance of the both MIR internal odometry and the speckle odometry were better when the robot traversed the square in the clockwise direction, this may be due to the presence of less features in the first side which was open corridor space, resulting in worse orientation estimation which is used by both methods in the calculation of position.

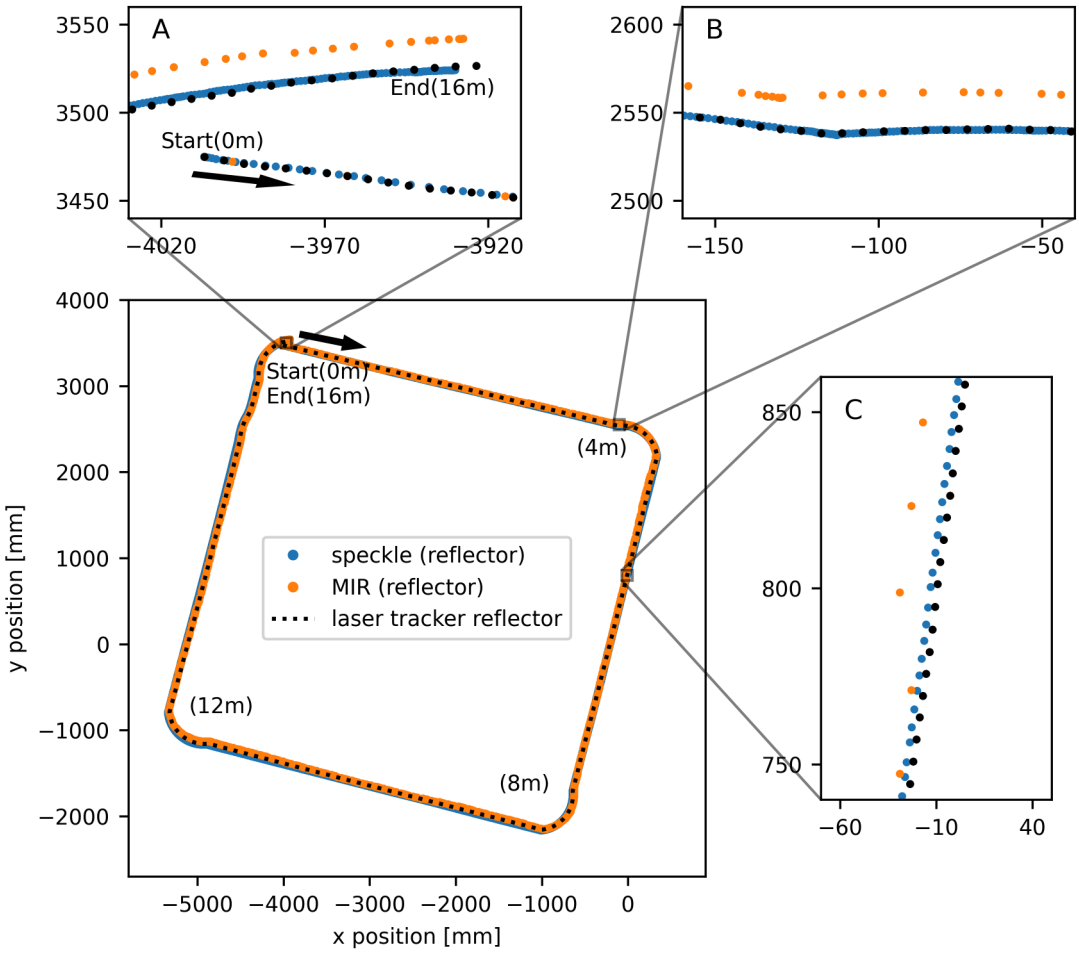

Figure 5: Comparison of position in laser tracker reflector frame for a 4m square path traversed in the clockwise direction, starting in the top-left (as indicated by arrow). Zoom A shows the starting and final positions, zoom B shows the positions at the end of the first side (4m) where the speckle odometry is significantly closer to position as measured by the laser tracker. Zoom C shows a correction adjustment made to the MIR odometry leading to a jump in reported velocity as show in Figure 4.

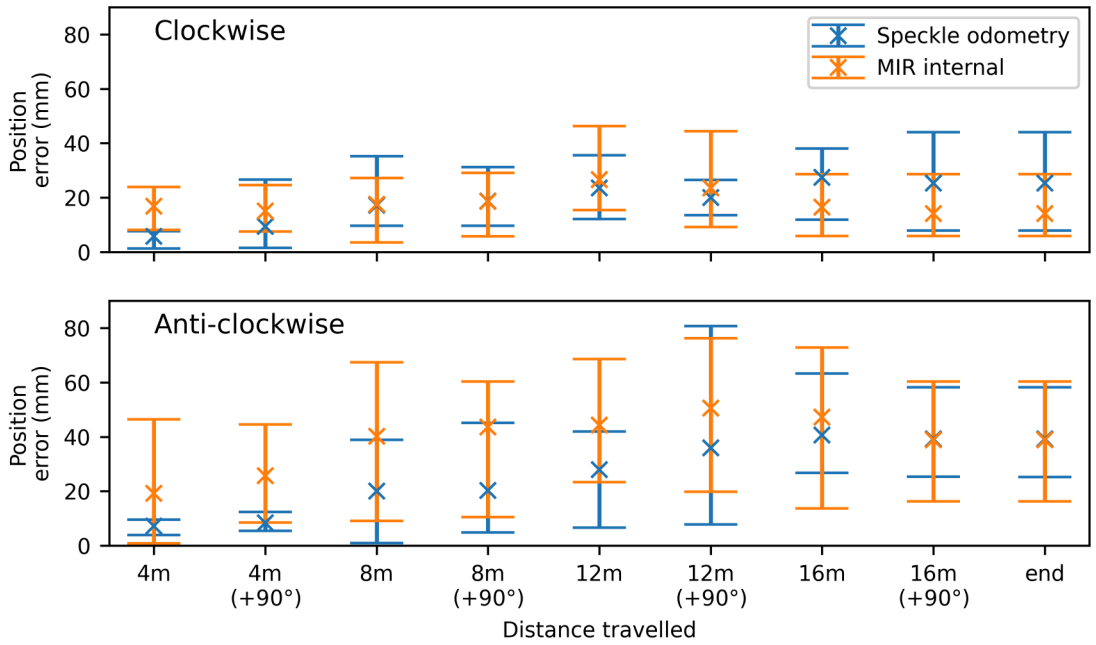

Figure 6: Calculated odometry errors at each corner, and after each rotation, in comparison to reference laser tracker measurements. Here data points show mean position error of six runs around a 4m square path in both clockwise (top) and anti-clockwise directions (bottom). The error-bars show the minimum and maximum observed error.

4. CONCLUSIONS

This paper reports the application of a laser speckle velocimetry sensor to a mobile industrial robot operating in a typical factory floor environment. The suitability of different floor surfaces was assessed in terms of the ability to form speckle patterns with sufficient signal to noise for correlation-based processing with all tested surfaces found to be suitable. The measured robot velocities, of up to 250mm/s were found to agree well with the robots internal SLAM/wheel encoder measurements to within < 0.3mm/s with the additional benefits of detecting both in-plane velocity components and the ability to resolve smaller speed fluctuations. The output of the speckle sensor was then used to calculate the robot's position with trial motions consisting of a 4m side square path; these were used to assess the performance and make a comparison with both the robot's internal SLAM/wheel encoder based odometry and also to reference position measurements made using a laser tracker. The results show comparable performance between the robot's internal SLAM/wheel encoder based odometry and the speckle odometry with errors in both of up to 80mm and significantly better when travelling in the clockwise directions. This may be related to the sparsity of features on the initial sides when travelling anti-clockwise leading to poor orientation measurement, which will affect the calculation of position from both methods. Even so, the speckle odometry performed significantly better over these initial sides, with a maximum error of < 10mm after 4m travel compared to < 47mm for the internal odometry, suggesting that speckle odometry may be useful in improving the quality of SLAM mapping.

ACKNOWLEDGMENTS

The authors would like to acknowledge The Manufacturing Technology Centre (MTC), Coventry, UK for their assistance. This work was supported by the Engineering and Physical Sciences Research Council (EPSRC) UK, (grant EP/S01313X/1). T.O.H.C. acknowledges the support of a RCUK Catapult Researchers in Residence award (EP/R513519/1).

REFERENCES

[1] Vaher, K., Kangru, T., Otto, T., and Riives, J., "The mobility of robotised work cells in manufacturing," *Annals of DAAAM and Proceedings of the International DAAAM Symposium* **30**(1), 1049–1055 (2019).

[2] Tao, B., Zhao, X. W., and Ding, H., "Mobile-robotic machining for large complex components: A review study," *Science China Technological Sciences* **62**(8), 1388–1400 (2019).

[3] Lachmayer, L., Recker, T., Dielemans, G., Dörfler, K., and Raatz, A., "Autonomous Sensing and Localization of a Mobile Robot for Multi-Step Additive Manufacturing in Construction," *International Archives of the Photogrammetry, Remote Sensing and Spatial Information Sciences - ISPRS Archives* **43**(B1-2022), 453–458 (2022).

[4] Helmberger, M., Morin, K., Berner, B., Kumar, N., Cioffi, G., and Scaramuzza, D., "The Hilti SLAM Challenge Dataset," *IEEE Robotics and Automation Letters* **7**(3), 7518–7525 (2022).

[5] Motroni, A., Buffi, A., and Nepa, P., "Mobile-robots indoor tracking and navigation: perspectives for rfid technology," *2022 7th International Conference on Smart and Sustainable Technologies (SpliTech)* , 1–6, IEEE (7 2022).

[6] Francis, D., Charrett, T. O., Waugh, L., and Tatam, R. P., "Objective speckle velocimetry for autonomous vehicle odometry.," *Applied Optics* **51**(16), 3478–90 (2012).

[7] Saito, R., Nagai, I., and Watanabe, K., "Motion estimation of a walking robot based on laser speckle odometry," *International Journal on Smart Material and Mechatronics IJSMMVol. 2 No. 2 2015* **2**, 94–97 (2015).

[8] Paijens, A. F., Huang, L., and Al-Jumaily, A. M., "Implementation and calibration of an odometry system for mobile robots, based on optical computer mouse sensors," *Sensors and Actuators, A: Physical* **301**, 111731 (2020).

[9] Mobile Industrial Robots A/S, "Mir200 user guide." https://supportportal.mobile-industrial-robots.com/documentation/mir200-manuals/mir200-user-guides-and-quick-starts. (Accessed: June 2023).

[10] Charrett, T. O., Kissinger, T., and Tatam, R. P., "Workpiece positioning sensor (wPOS): A three-degree-of-freedom relative end-effector positioning sensor for robotic manufacturing," in [*Procedia CIRP*], **79**(July), 620–625, Elsevier B.V. (2019).

[11] Goodman, J. W., [*Speckle phenomena in optics: theory and applications*], SPIE Press, Bellingham, WA (2007).

https://dspace.org/

Application and performance of laser speckle odometry applied to a mobile industrial robot

Charrett, Thomas O. H.; Gibson, Sam; Tatam, Ralph P.

2023-08-15
SPIE - International Society for Optics and Photonics
https://doi.org/10.1117/12.2673177
Charrett TOH, Gibson SJ, Tatam RP. (2023) Application and performance of laser speckle odometry applied to a mobile industrial robot. In: SPIE Optical Metrology 2023: Optical Measurement Systems for Industrial Inspection XIII, 26-29 June 2023, Munich, Germany, Proceedings of SPIE, Volume 12618

Downloaded from a DSpace repository. https://dspace.org/